J Mol Model (2007) 13:485–497
DOI 10.1007/s00894-006-0164-5

ORIGINAL PAPER

Cold-active enzymes studied by comparative molecular dynamics simulation

Vojtěch Spiwok · Petra Lipovová · Tereza Skálová · Jarmila Dušková · Jan Dohnálek · Jindřich Hašek · Nicholas J. Russell · Blanka Králová

Received: 7 September 2006 / Accepted: 2 November 2006 / Published online: 18 January 2007

Abstract Enzymes from cold-adapted species are significantly more active at low temperatures, even those close to zero Celsius, but the rationale of this adaptation is complex and relatively poorly understood. It is commonly stated that there is a relationship between the flexibility of an enzyme and its catalytic activity at low temperature. This paper gives the results of a study using molecular dynamics simulations performed for five pairs of enzymes, each pair comprising a cold-active enzyme plus its mesophilic or thermophilic counterpart. The enzyme pairs included α-amylase, citrate synthase, malate dehydrogenase, alkaline protease and xylanase. Numerous sites with elevated flexibility were observed in all enzymes; however, differences in flexibilities were not striking. Nevertheless, amino acid residues common in both enzymes of a pair (not present in insertions of a structure alignment) are generally more flexible in the cold-active enzymes. The further application of principle component analysis to the protein dynamics revealed that there are differences in the rate and/or extent of opening and closing of the active sites. The results indicate that protein dynamics play an important role in catalytic processes where structural rearrangements, such as those required for active site access by substrate, are involved. They also support the notion that cold adaptation may have evolved by selective changes in regions of enzyme structure rather than in global change to the whole protein.

Keywords Cold-active enzymes · Psychrophiles · Extremophiles · Molecular dynamics · Flexibility

Electronic supplementary material Supplementary material is available in the online version of this article at http://dx.doi.org/10.1007/s00894-006-0164-5 and is accessible for authorized users.

V. Spiwok (✉) · P. Lipovová · B. Králová
Department of Biochemistry and Microbiology,
Institute of Chemical Technology Prague,
Technická 5,
Prague 6 166 28, Czech Republic
e-mail: spiwokv@vscht.cz

T. Skálová · J. Dušková · J. Dohnálek · J. Hašek
Institute of Macromolecular Chemistry,
The Academy of Sciences of the Czech Republic,
Heyrovského nám.2,
Prague 6 162 06, Czech Republic

N. J. Russell
Department of Agricultural Sciences, Imperial College London,
Wye campus,
Ashford, Kent TN25 5AH, UK

Introduction

Enzymes from thermophilic and hyperthermophilic organisms are applied in biotechnologies at scales ranging from large biotechnological processes to nano-scale PCR reactions. The benefits arising from the fact that these enzymes are stable at elevated temperatures are invaluable. On the other hand, application of enzymes from cold-adapted organisms (e.g. psychrophilic bacteria) possesses advantages for low-temperature biotechnologies. Enzymes from mesophilic and thermophilic organisms usually remain in a native conformation at low temperature but their activity is significantly suppressed. Enzymes from species living at low temperatures - cold-active enzymes - are adapted to perform their catalytic function at low temperatures (viz. 0–10 °C) and therefore they are more suitable for low-temperature biotechnological applications.

This can be illustrated by the example of cold-active xylanase from family 8 of the glycosyl hydrolase classification [1]. At 10 °C, the enzyme from the Antarctic

bacterium *Pseudoalteromonas haloplanktis* is approximately 8 times more active than the mesophilic family 11 xylanase from *Streptomyces* sp. S38 and approximately 130 times more active than the thermophilic endoglucanase from *Clostridium thermocellum* for the same substrate (compared as k_{cat}) [1]. In other words, it is necessary to use approximately 8 times higher amount (in molar and approximate mass terms) of mesophilic and approximately 130 times higher amount of thermophilic enzyme to obtain the same catalytic effect. Nonetheless, the activities of these enzymes at their apparent optimal temperatures are comparable. This concords with the fact that optimal growth rates of psychrophilic, mesophilic and thermophilic microorganisms are not markedly different, only shifted in temperature [2].

The mechanism of enzyme adaptation to function at low temperature is not fully understood. Several structural features of cold-active enzymes have been observed based on crystal structures [3–11], homology models [11, 12] and a comparative genomic study [13]. These features include a reduced number of salt bridges, a lower [Arg/(Arg+Lys)] ratio, a reduced number of buried non-polar residues, a higher number of exposed non-polar residues, a higher number of exposed glutamine residues, higher number of glycines in loops, and a reduced content of proline in cold-active enzymes. Most of these features are in agreement with our knowledge of protein stability and folding; nevertheless, the physical basis of their impact on activity at low temperature remains an open issue.

The concept of an inverse relationship between activity and stability has often been proposed (e.g. [14]). Cold-active enzymes are proposed to retain high conformational flexibility at low temperature. According to this theory, a higher conformational flexibility is a rationale for higher activity, but concomitantly it causes a reduced stability of these enzymes. Several studies addressing the issue of stability-activity relationships have been reported in recent years on cold-active as well as meso- and thermophilic enzymes. For example Shoichet and co-workers showed that in both T4 lysozyme and β-lactamase catalytic amino acid residues have evolved for activity rather than for stability [15, 16]. Mutation of key catalytic residues leads to reduced or abolished activity, whereas stability was increased. Several molecular modelling studies also address this issue. For example comparative molecular dynamics (MD) study of Atlantic cod and human uracil DNA glycosidases and their mutants showed that mobility of the substrate-recognizing loop correlates with activity at low temperature (expressed as k_{cat}/K_m) [17].

In contrast, the reduced stability of enzymes from cold-adapted species could also result from the lack of an evolutionary pressure for stability without any role of activity. Using the lattice model, Taverna and Goldstein showed that the reason why most proteins are marginally stable (i.e. unstable at temperatures higher than the physiological) is due to a lack of pressure for thermostability [18]. This typical property of proteins - i.e. marginal thermostability - is a result of the fact that proteins are highly complex entities. Simulation of molecular dynamics of trypsin from cold-adapted fish did not reveal any significant difference in flexibility when compared with its mesophilic counterpart [19, 20]. An electrostatic term of enzyme-substrate interaction rather than flexibility was proposed to be a rationale of its higher activity [21, 22]. This proposal was further supported by calculation of the free energy of enzyme-substrate interaction using a linear interaction energy method [23]. Optimization of electrostatic properties of the active site of Atlantic cod uracil DNA glycosidases was also proposed to play an important role in activity at low temperature [24].

Activity-stability and activity-flexibility relationships can be also studied using site-directed mutagenesis and directed evolution techniques. A disadvantage of comparing enzymes from different organisms is that we cannot directly distinguish between evolutional phylogenetic changes that are responsible for activity at low temperatures and those that are responsible for other features or represent an evolutional drift. Using enzyme engineering techniques, one can determine whether single or several residues are responsible for activity at low temperature. Some data from these techniques support the idea of an inverse stability-activity relationship, in that mutants active at low temperature are also less stable at elevated temperature [25–27], whereas other show the opposite trend [28, 29].

The question arises as to how much important is protein dynamics in enzyme catalysis. Thermal fluctuations similar to that present in enzyme structure are also present in non-enzymatic reactions. The concept of collective motions in protein structure, which promote enzyme function seems promising in answering this question and is currently supported by theoretical as well as experimental methods ([30] and references within).

Molecular dynamics simulation was one of first methods that showed proteins to be dynamic entities [31]. It can explore dynamical properties of proteins over a wide range of frequencies and amplitudes. Application of simulation of molecular dynamics was successful in observing the dynamic transition of protein [32] and in interpreting of crystallographic B-factors [33]. As far as we know, the only application of molecular dynamics simulation to the issue of adaptation to low temperature is a comparative molecular dynamics simulation of salmon and bovine trypsins [19, 20] and on Atlantic cod uracil DNA glycosylase [17]. Several comparative molecular dynamics studies have been reported for thermophilic enzymes [34–36].

In this paper we present the results of a molecular dynamics study of five cold-active enzymes, together with

five homologues from meso- or thermophilic sources. Total 1–1.4 ns trajectories were calculated for the enzymes in explicitely solvated systems. We examined the fluctuations of atoms as root-means square fluctuation (RMSF). An essential dynamics analysis (principal component analysis, harmonic dynamics) was also performed [37]. This type of analysis enabled the molecular motions to be "dissected" into a limited number of collective motions and therefore to reduce the dimensionality of the problem.

Methods

The X-ray structures of five cold-active enzymes were selected from the protein databank (PDB) [38]. They include a majority of cold-active enzymes that have been structurally studied, but for which no comparative molecular dynamics study have been reported. Similar comparative molecular dynamics studies were documented for fish trypsins [19, 20] and uracil DNA glycosylase [17]. The choice of meso- or thermophilic counterparts from the PDB was based on their similarity with corresponding cold-active enzymes and by resolution of their structure. The level of structural similarity was measured as the root-mean-square deviation (RMSD) of C^{α} atoms and by identity of amino acid sequence. Combinatorial extension (CE) [39] was used as a structural alignment tool. The selected enzymes are listed in Table 1 and illustrated in Fig. 1. Corresponding X-ray structures are listed in Table 2.

Missing amino acid residues in the cold-active alkaline protease (Apr_P, residues 184–188) were added by using a simple homology modelling procedure. Briefly, the full length structure was obtained using the program Modeler [40] based on the original structure from the PDB as a template. If side-chains were missing in published structures, they were added using the SQWRL program [41]. The N-terminal pyroglutamic acid residue in Amy_M (Table 1) was removed prior to simulation. Because the structure of citrate synthase from *Arthrobacter* sp. DS2-3R is deposited in the PDB as a monomer, the dimer structure was obtained by symmetry operation following instructions in the header of the PDB record.

All substrates and coenzymes were deleted prior to simulation. The role of certain ions in α-amylases [42] and alkaline proteases [43] have been extensively studied. We decided, therefore, to retain all calcium ions in simulations of both alkaline proteases and a calcium cation and a chloride anion in the α-amylases. Those water molecules in the PDB files that were strongly bound to a structure of an enzyme were included. The decision as to which water molecules were included was driven by their B-factor values and by visual inspection (buried water molecules and water molecules in the vicinity of the protein surface were included). B-factor cut-offs were different from structure to structure because values of B-factor depend on technical details of X-ray data measurement and model refinement.

Table 1 Enzymes studied in this study

Enzyme	Organism	Abreviation
α-amylase	*Pseudoalteromonas haloplanktis*	Amy_P
	pig	Amy_M
citrate synthase	*Arthrobacter* sp. DS2-3R	Cit_P
	Pyrococcus furiosus	Cit_H
malatedehydrogenase	*Aquaspirillum arcticum*	MDH_P
	Thermus thermophilus Hb8	MDH_H
alkaline protease	*Pseudomonas* sp.	Apr_P
	Pseudomonas aeruginosa	Apr_M
xylanase	*Pseudoalteromonas haloplanktis*	Xyl_P
	Clostridium thermocellum	Xyl_T

The first enzyme in each pair is cold-active and the second is from a meso- or thermophilic source. The second part of the abreviation indicates whether the enzyme comes from a psychrophilic (P), mesophilic (M), thermophilic (T) or hyperthermophilic (H) organism.

Each enzyme was solvated by putting it into a water box generated from replicas of SPC216 water [44]. The size of each box was set so that a minimal distance between a solute and a side of the box was 0.8 nm. A total number of water molecules in a box ranged from 10 152 for the thermophilic xylanase to 23 842 for thermophilic the citrate synthase. We used protonation states of Lys, Arg, Glu and Asp corresponding to neutral pH. Protonation states of His were optimized for H-bond networks. Protonation states of histidine residues in metal-chelating sites were assigned based on visual inspection. Each ensemble was then minimized using steepest-descent minimizer. Molecular dynamics was simulated in NPT ensemble (conserved number of atoms, pressure and temperature) using the Gromacs 3.1.4 package [45, 46] in Gromacs (united atom) force field. Temperature and pressure were set to 300 K (unless otherwise stated) and 1 bar using the Berendsen thermostat [47] and the Parrinello-Rahman barostat [48], respectively. The LINCS algorithm [49] was used to constrain all bonds. A cut-off for electrostatic and van der Waals interactions was set to 1.4 nm. A time-step was set to 2 fs and a trajectory was sampled every 2 ps. For xylanases 1.4 ns trajectories were calculated, because xylanases are smaller than the other studied enzymes, in order to make the simulations less time-consuming. Each trajectory was comprised of an equilibration phase (200 ps) and a production phase (800 or 1'200 ps).

Simulation of molecular dynamics was monitored using RMSD during dynamics simulation (minimized structure used as a reference, see supplementary material). Root-

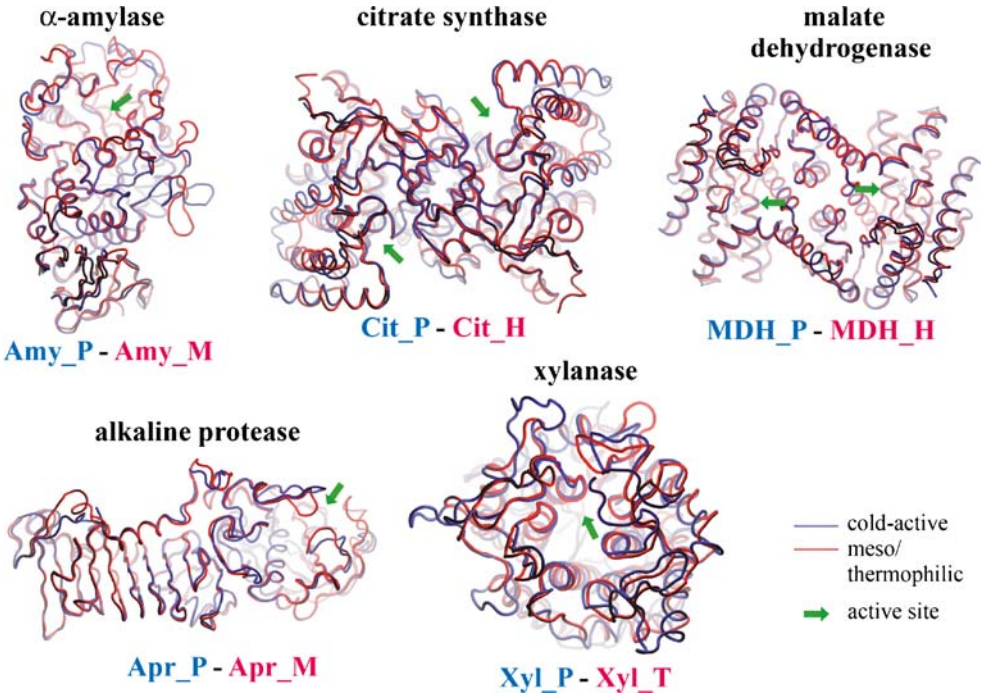

Fig. 1 Studied enzymes aligned by the CE method. Cold-active enzyme is shown in blue; the enzyme from meso- or thermophilic source is in red. Active-site residues are showed as spheres (zinc is the green ball in structures of alkaline proteases)

mean-square fluctuations (RMSF) were calculated for protein C^{α} atoms. The first 200 ps (equilibration phase) was omitted from each trajectory in RMSF calculations. The RMSF calculation was performed in short as well as long time-scales. The former was performed for 16 separated 50 ps windows (24 separated 50 ps windows for xylanases) and then averaged. The latter RMSF calculation was performed for a whole production trajectory. RMSD and RMSF values were calculated for each monomer of dimeric enzymes (citrate synthases and malate dehydrogenases). The overall RMSF value of protein atoms was calculated by averaging the RMSF values for C^{α} atoms over time as well as a polypeptide chain using the relationship:

$$RMSF = \sqrt{\frac{1}{N_{atoms} n_{frames}} \sum_{frames} \sum_{atoms} |\mathbf{r} - \langle \mathbf{r} \rangle|^2}$$

where **r** and <**r**> are actual and time-averaged vectors, respectively, of Cartesian coordinates of the atom. Aligned RMSF plots (Fig. 2) were obtained by juxtaposition of one RMSF plot on another based on CE sequence alignment [39].

Essential dynamics analysis was performed using the Gromacs 3.2.1 package for C^{α} atoms. In the first step, the structures of enzymes are superimposed by their C^{α} atoms and a time-averaged structure is calculated (number of C^{α} atoms is N). Then, a covariance matrix is calculated as $C_{ij} = \left\langle (x_i - \langle x_i \rangle)(x_j - \langle x_j \rangle)^T \right\rangle$ for superimposed coordinates (i=1 to $3N$). The covariance matrix is then diagonalized. Eigenvalues correspond to an extent of a motion and eigenvectors correspond to directions of motions of individual atoms. Analysis was performed for production trajectories of each studied enzyme (the first 200 ps were omitted from a trajectory). Dimer enzymes were analyzed as a single system.

Table 2 Structures of the investigated enzymes

Enzyme	PDB ID	Resolution (Å)	R-value	Number of amino acids in structure	Ligands	Sequence identity (%)	Reference
Amy_P	1AQM	1.85	0.157	448	Ca^{2+}, Cl^{-}	50.7	[2]
Amy_M	1HX0	1.38	0.108	495	Ca^{2+}, Cl^{-}		[61]
Cit_P	1A59	2.09	0.184	2×377	–	39.3	[3]
Cit_H	1AJ8	1.90	0.191	2×371	–		[62]
MDH_P	1B8P	1.90	0.175	2×327	–	62.5	[4]
MDH_H	1IZ9	2.00	0.193	2×327	–		[63]
Apr_P	1G9K	1.96	0.156	461	Zn^{2+}, Ca^{2+}	55.3	[5]
Apr_M	1KAP	1.64	0.176	470	Zn^{2+}, Ca^{2+}		[64]
Xyl_P	1H12	1.20	0.108	404	–	23.0	[6]
Xyl_T	1CEM	1.65	0.162	363	–		[65]

Sequence identities were calculated using the CE program [39].

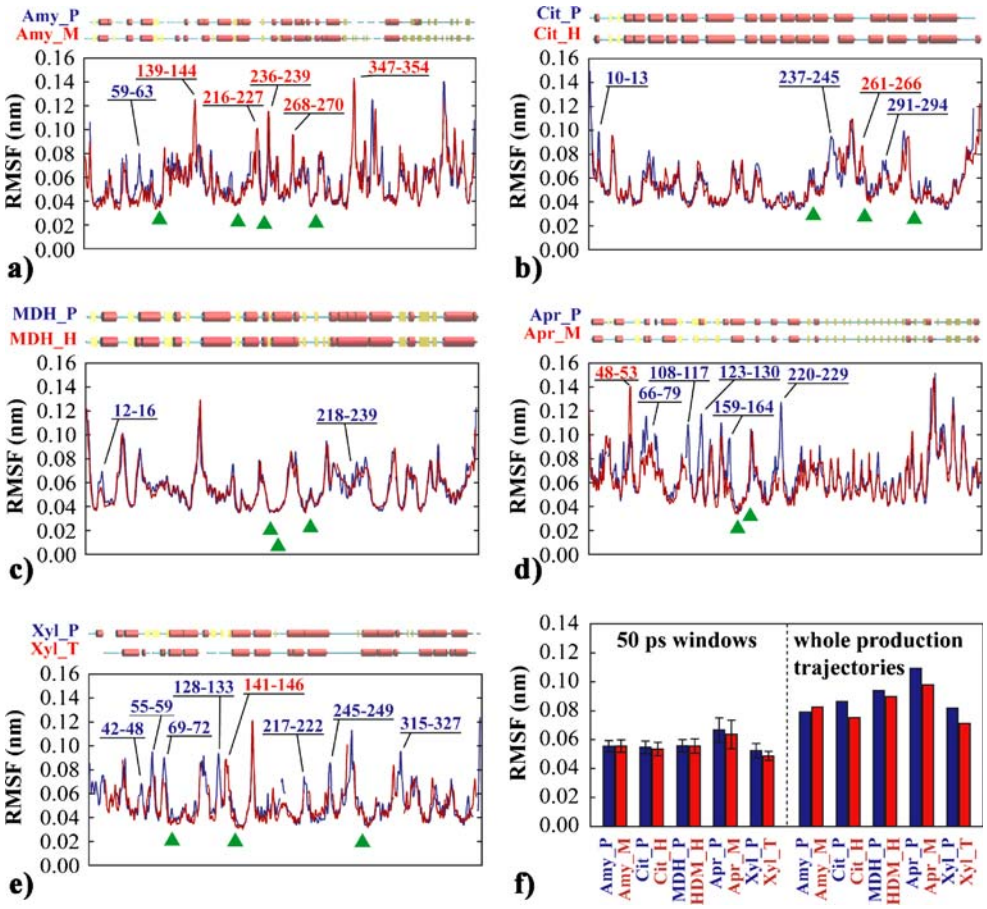

Fig. 2 Flexibility profiles of studied enzymes defined as RMSF calculated for snapshots in 50 ps windows. (**a**) α-amylases. (**b**) citrate synthases. (**c**) malate dehydrogenases. (**d**) alkaline proteases. (**e**) xylanases. Cold-active enzymes are shown in blue; enzymes from meso- or thermophilic proteins in red. Secondary structure from N-terminus to C-terminus is illustrated for each flexibility profile. Active site residues are illustrated by green triangles. (**f**) Residue-averaged flexibilities calculated in 50 ps windows or a whole production trajectory

Results and discussion

Model structures

Five enzymes were selected on the basis of their sequence homology in the pair and for the quality of their X-ray structures (resolution, R-value etc.), namely α-amylase, citrate synthase, malate dehydrogenase, alkaline protease and xylanase. In each pair, one enzyme originated from a psychrophilic and one enzyme originated from a meso- or thermophilic organism. These enzymes are listed in the Table 1 and illustrated in Fig. 1. Structures selected for this study cover a wide range of protein folds. The sequence identity in pairs of structures was between 23 and 63%. Monomeric as well as oligomeric (dimeric) enzymes were studied. The selected enzymes included some which contained metal ions as cofactors.

Performance of molecular dynamics simulation

Deterministic (Newtonian) molecular dynamics simulation (duration 1–1.4 ns) was performed for all studied enzymes. Simulation was performed in NPT ensemble with explicit solvent. Minimized experimental X-ray structures were used as an initial state of simulation. The overall performance and representative nature of molecular dynamics simulation was evaluated taking into account the profiles of RMSD as a function of time, by visual inspection of trajectories, secondary structure stability and by comparison of calculated RMSF profiles with experimental B-factor profiles. Conformational changes during a steepest descent energy minimization did not exceed 0.03 nm (RMSD of all atoms). During the production phase of simulation, values of RMSD for C^{α} atoms (difference between current and initial coordinates) fluctuated around a certain value (see supplementary material). These values did not exceed 0.35 nm, which can be interpreted as being representative of a stable system. Maximal values of RMSD were typically higher for multi-domain, less compact enzymes (e.g. alkaline proteases or dimeric enzymes) and lower for rather compact single-domain enzymes (e.g. xylanases). There was no evidence of splitting or rearrangement of a subunit assembly in the four dimeric enzymes. The relationship between the maximal value of RMSD and resolution of an X-ray structure used as an initial model was carefully evaluated, because low resolution structures and NMR models have been reported to diverge more from the initial model during the time-course of a molecular dynamics simulation [50]. Yet, there was no observable relationship between maximal values of RMSD and the

resolution of an X-ray structure used as an initial model. There was also no significant relationship between the maximal value of RMSD and the number of water molecules in the crystal structure included in the simulation. These observations prove that the results of this study were unaffected by differences in structural resolution of structures used as an initial model. The stability of interactions between metal ions and proteins were examined by profiles of RMSD as a function of time, as well as by visual inspection. No significant rearrangements were observed for ion-protein interactions, except for interaction of the mesophilic alkaline protease (Apr_M) and the calcium cation 615 at the late stage of the simulation (the number corresponds to that of the PDB file). Affinities of different calcium-binding sites in the cold-active alkaline protease (Apr_P) have been studied by X-ray crystallography [43]. Results of the presented study indicate that the calcium ion released during simulation of Apr_M is bound rather weakly in this family of alkaline proteases.

Flexibility profiles

Comparisons of RMSF profiles constructed on the basis of structure-structure alignments for individual enzyme pairs are illustrated in Fig. 2 (3D structures color-scaled by RMSF can be obtained as supplementary material). As expected, rigid parts of proteins were located in core, whereas flexible parts were located mainly in loops. The level of similarity between RMSF profiles of the enzymes within a pair was closely related to their sequence homology. Malate dehydrogenases with the highest sequence homology and almost no insertions/deletions showed minimal differences in RMSF profiles. In contrast, insertions/deletions in α-amylases showed high RMSF values for insertions in the cold-active as well as the mesophilic enzyme. Differences in the flexibilities of certain regions of individual enzymes are discussed below.

Essential dynamics

Overall in the studied enzymes there were 6–17 eigenvectors with corresponding eigenvalues higher than 0.05 nm^2, i.e. sufficient to describe motions of a protein at a reasonable accuracy. This is in agreement with other essential dynamics studies of globular proteins [37]. In order to elucidate whether a certain eigenvector corresponded to analogous movements in both enzymes of a pair, movements associated with the individual eigenvector (typically the first and the second) were visually examined and compared for both enzymes. In addition, for each snapshot the projection of a trajectory on an eigenvector was calculated. Time-development of a conformational change associated with a given eigenvector was compared between a cold-active enzyme and an enzyme from a meso- or thermophilic organism by calculation of correlation and regression coefficients (time-development of projection in a meso- or thermophilic enzyme versus time development of projection in cold-active enzyme). A time-development of projections of a trajectory of Cit_P and Cit_H on their first eigenvectors are illustrated in Fig. 3a and b, respectively. Correlation of these two projections is illustrated in Fig. 3c. If there was a strong negative correlation, the value of one of projections of a trajectory on an eigenvector was multiplied by −1 to get a positive correlation. This is possible due to the fact that a vector opposite to an eigenvector is also a solution of an eigenproblem. A strong correlation between the time-development of projection in a meso/thermophilic and a psychrophilic enzyme indicates that motions associated with this eigenvector are analogous. This was further tested by visual inspection of a trajectory from which motions associated with the given eigenvector were filtered. Similarly, the value of the regression coefficient indicates whether the motion associated with a given eigenvector is enhanced or suppressed in one enzyme of a pair. A value of the regression coefficient lower than 1 indicates a higher amplitude or rate of this motion in the cold-active enzyme. The results of this analysis are given in Table 3.

Comparison of enzyme pairs

α-Amylase

The X-ray structure of α-amylase from *Pseudoalteromonas haloplanktis* was the first published for a cold-active enzyme. Pig α-amylase was selected as a mesophilic counterpart. Figure 2 shows that there is only a single region with slightly higher RMSF values in the cold-active α-amylase (residues 59–63) whereas five regions with significantly higher RMSF are present in the mesophilic α-amylase (residues 139–144, 216–227, 236–239, 268–270 and 347–354). Only one of these regions with elevated flexibility (residues 236–239 in Amy_M or residues 203–206 in Amy_P) is common to both enzymes, while others correspond to insertions. Moreover, this more flexible region is located in the vicinity of the substrate binding site. We anticipate that the large number of highly flexible loops in the mesophilic (porcine) α-amylase is due to a different nature of evolution in prokaryotic and eukaryotic enzymes. Prokaryotic evolutionary changes are dominated by single point mutations whereas those in eukaryotes are dominated by recombinations. The fact that eukaryotic proteins tend to contain more loops than prokaryotic was reported [51]. Unfortunately, to the best of our knowledge, there is no available X-ray structure of prokaryotic α-amylase with a reasonable similarity to α-amylase from *P.*

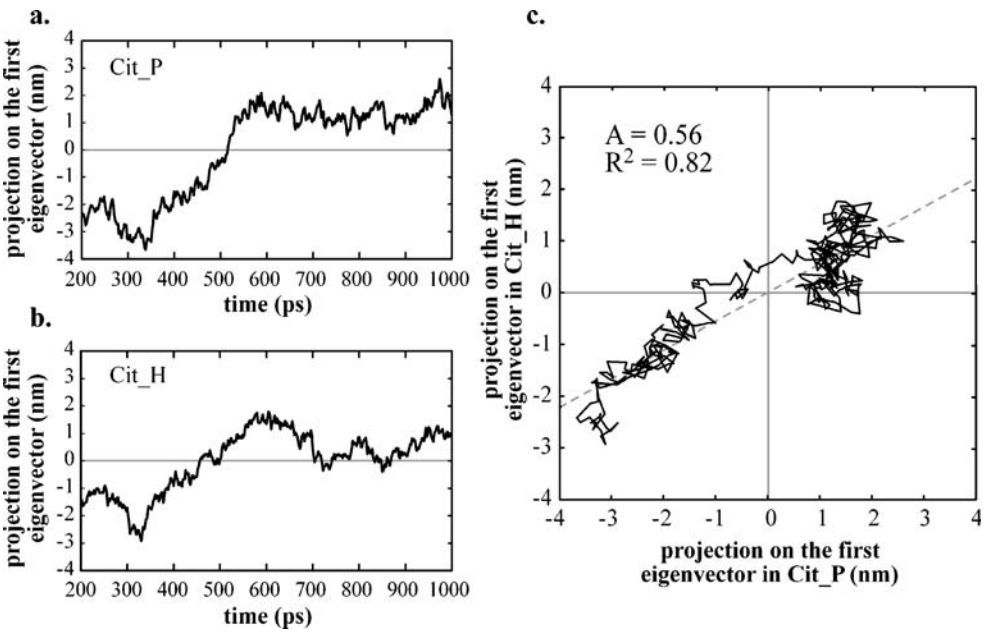

Fig. 3 Projection of the first eigenvector to a trajectory. (**a**) the trajectory of the cold-active citrate synthase. (**b**) the trajectory of the hyperthermophilic citrate synthase. (**c**) their correlation indicates whether motions associated with the eigenvectors are analogous and whether they are enhanced in one enzyme of the pair

haloplanktis (Amy_P). Comparison of RMSF profiles of the two enzymes shows that mesophilic α-amylase is more flexible due to presence of numerous insertions. A role for these loops in catalysis or stability is not evident. The study of closely related α-amylases from *Bacillus licheniformis* (thermostable) and *Bacillus amyloliquefaciens* (less thermostable) revealed that the thermostable one is more flexible as measured by H/D exchange and neutron scattering experiments [52]. Moreover, these enzymes are highly homologous with only a single short insertion. The

Table 3 Results of essential dynamics analysis

Enzyme	PC #	Eigenvalue (% of sum of eigenvalues)		A	R^2	Structural motions
		cold-active	meso-/thermophilic			
α-amylase	1	23	31	1.22	0.81	bending, opening/closing of active site, in Amy_M, also movements of loop of residues 138–152, 346–355
	2	13	12	0.82	0.52	bending, movements of loop (residues 136–146) in Amy_P, movements of loop (residues 235–243) in Amy_M
citrate synthase	1	35	21	0.56	0.82	opening/closing of citrate-binding region of the active site and CoA-binding cleft
	2	17	15	0.28	0.15	opening/closing of CoA-binding cleft
malate dehydrogenase	1	41	51	0.97	0.85	opening/closing of the active site, movements of the loop of (residues 91–97) in MDH_H
	2	19	12	0.65	0.73	dimer bending
alkaline protease	1	31	29	0.66	0.56	bending, active site movements
	2	16	12	0.39	0.24	bending of Apr_M, active site movements
xylanase	1	35	20	0.56	0.88	opening of active site, also in Xyl_P movements of residues 66–72 and 375–379
	2	10	18	0.98	0.80	movement of the whole $(\alpha/\alpha)_6$ fold in both enzymes

Proportion of motions associated with a given eigenvector on total motions is given. Projection of trajectories on selected eigenvectors was calculated for each enzyme. Regression (A) and correlation (R^2) coefficients for the projection of the trajectory on the eigenvector in meso- or thermophilic versus the projection of the eigenvector in cold-active enzyme are presented with corresponding structural meaning. High correlation coefficients indicate that these motions are analogous; a regression coefficient lower than 1 indicates that motions are enhanced in the cold-active enzyme.

authors of this study proposed a rise of conformational entropy for the thermostable enzyme as a rationale of stabilization.

For trajectories of α-amylases, essential dynamics analysis was performed. The profiles of time development of the first and the second eigenvectors did not significantly differ between both α-amylases. Movements associated with the first eigenvector were characterized by overall bending of the structure accompanied by opening and closing of the active site. Moreover, in the mesophilic enzyme (Amy_M), large movements of loops of residues 138–152 and 347–355 were associated with the first eigenvector. These regions were also observed to be more flexible from RMSF profiles. Conformational changes associated with the first eigenvector were higher in the mesophilic α-amylase as indicated by the regression coefficient of projection on the first eigenvector of both enzymes. There was a weaker relation between motions associated with the second eigenvector for the two enzymes. Movement associated with the second eigenvector was characterized by structure bending. In the cold-active enzyme, movements of the region of residues 136–146 corresponding to the second eigenvector were slightly enhanced. This region forms the binding site. On the other hand, movements of residues 235–243 were enhanced along the second eigenvector in the mesophilic enzyme. These results are in agreement with a flexibility calculated as RMSF profiles and indicate that higher flexibility of the mesophilic enzyme is caused by the presence of a large number of loop regions. Their role in adaptation to function at low/high temperature is not clear.

Citrate synthase

Citrate synthase from *Arthrobacter* sp. DS2-3R and its archaeal hyperthermophilic homolog were selected as a second pair. Citrate synthase is a dimeric enzyme with an active site that is covered by a closing domain, which undergoes large conformational movements during opening and closing of the active site. This opening was also clearly visible during a molecular dynamics simulation and is in agreement with the molecular dynamics study of Rocattano and co-workers [53]. There are three regions in the flexibility profiles of citrate synthases with elevated RMSF values for the cold-active enzyme (Fig. 2). Slightly higher flexibility in the region close to the active site in cold-active citrate synthase (residues 10–13) was detected. Two other regions with high flexibility in the cold-active citrate synthase are located in loops (residues 237–245 and 291–294). They both seem to play an important role in catalysis. Residues 237–245 are likely to control the opening/closing rate of the active site. There was only one region with elevated flexibility in the thermophilic enzyme (residues 261–266) and this region is a part of the active site. Larger structural differences were also present in the N- and C-termini, which are not expected to play an important role in cold adaptation.

In citrate synthase, the movements associated with the first and the second eigenvectors were characterized by domain opening and closing. Along the first eigenvector, movements were characterized by opening of the citrate-binding (interior) active site as well as by opening of the CoA-binding cleft. Movements along the second eigenvector were characterized only by opening of CoA-binding cleft. Nevertheless, the extent of this opening during the simulation is lower than the full opening required during the catalytic cycle of the enzyme. In both enzymes the extent of opening was higher for one of the two monomers. There was a strong correlation between time development of the first eigenvector of the two enzymes (R^2=0.82), whereas movements along the second eigenvector were poorly correlated (R^2=0.15). Motions along the first and the second eigenvectors were enhanced in the cold-active enzyme according to regression of projections on eigenvectors for both enzymes. Opening and closing of the active site of the porcine citrate synthase (homologous to those studied herein) was intensively studied by Rocattano et al. using molecular dynamics simulation [53]. They showed that there are two main degrees of freedom associated with opening and closing of the binding site in agreement with our results. Kurz et al. showed that enzyme dynamics is the rate-limiting step of the reaction catalyzed by citrate synthase from the thermophile *Thermoplasma acidophilum* (homologous to citrate synthases studied in this study), whereas the rate-limiting step of mesophilic (porcine) citrate synthase is a substrate turnover step [54]. With respect to this study, it seems that the flexibility of psychro- and mesophilic citrate synthases is tuned to assure fluxes of substrates and products, whereas flexibility of thermo- and hyperthermophilic enzymes is reduced. This reduction in flexibility means that substrate/product fluxes are rate-limiting for the thermostable enzyme. The origin of this reduced flexibility could be either an evolutionary pressure for stability or a lack of evolutionary pressure for high activity.

Malate dehydrogenase

Malate dehydrogenase from the psychrophile *Aquaspirillium arcticum* and its archeal hyperhermophilic homolog were the third studied pair. They share the highest homology among all studied pairs of enzymes. There were no significant differences in RMSF profiles of malate dehydrogenases owing to the highest sequence homology and the presence of only a single insertion/deletion. Slightly elevated flexibility is found in the region of residues 12–16

of MDH_P in the vicinity of the active site (Fig. 2). There was a difference in the profile of the region that is comprised of two helixes (residues 218–239 in MDH_P and residues 214–234 in MDH_H). The profile of RMSF was smoother for the cold-active enzyme in this region.

In the malate dehydrogenases, movements along the first eigenvector were associated with opening and closing of the catalytic site. The extent of motions along the first eigenvector was comparable in both enzymes as shown by regression coefficient. Motions associated with the second eigenvector were characterized by overall bending of the dimer assembly. This bending was enhanced in the cold-active enzyme as shown by regression coefficient.

Alkaline protease

Extracellular alkaline proteases, from psychrophilic and from mesophilic *Pseudomonas* specie were selected for comparison. Alkaline protease has a rod-shaped structure composed of two main domains. The catalytic domain is the more spherical domain of mixed α/β secondary structure, whilst the non-catalytic domain is more rod-shaped with mainly β structure. Residues with elevated flexibility in the cold-active enzyme are found in six regions (residues 66–79, 108–117, 123–130, 159–164 and 220–229 in Apr_P) located in the catalytic domain (Fig. 2). Three of these regions contain insertions (residues 66–79, 106–115 and 219–228 in Apr_P). It should be noted that residues 111 and 112 are missing in the crystal structure of Apr_P and were modelled prior to MD simulation. Therefore, some artefacts might arise from modelling of this loop. Some of these loops are part of the active site (residues 123–130 in Apr_P) or located in the vicinity of the active site (residues 108–117 in Apr_P). On the other hand, there was only one region with elevated flexibility in the thermophilic enzyme (residues 48–53 in Apr_M). There were only minor differences in flexibilities of the non-catalytic domain.

The domain assembly of alkaline proteases is highly flexible and the structure undergoes bending motions during molecular dynamics simulation. Motions with the first and second eigenvectors in both alkaline proteases were associated with bending of the structure as well as by motions of loops in the active site region. However, the correlation between the two enzymes for the first and second eigenvalues was poor. Therefore, essential dynamics analysis for the catalytic (N-terminal) domain was performed. Only residues 20–245 for Apr_P and residues 18–248 for Apr_M were included for analysis. When the C-terminal domain was excluded, projection on the first and second eigenvectors between the two enzymes became more strongly correlated (see supplementary material). The first eigenvector showed regression coefficient A=0.98 and correlation coefficient R^2=0.89, indicating that the extent of these motions was almost equivalent. Movements of the active site were associated with the first eigenvector for catalytic domains of both enzymes. In the cold-active protease these movements were mainly located in residues 148–161 and 218–228, whereas in the mesophilic enzyme they represent the overall opening and closing of the active site. The second eigenvector showed regression coefficient A=0.67 and correlation coefficient R^2=0.67. Motions associated with the second eigenvector were characterized by opening and closing of the active site. In the cold-active enzyme this was associated with bending along the axis formed by the α-helix of residues 162–175. Therefore, not only flexibility but also modes of motions seem to be slightly different in these enzymes, despite their relatively high homology.

Xylanase

The level of sequence identity between the xylanases was the lowest among the studied enzyme pairs due to a number of insertions/deletions. The majority of sites with elevated flexibility correspond to insertions in one of the enzymes (Fig. 2). In the cold-active enzyme there were seven regions with significantly elevated flexibility (residues 42–48, 55–59, 69–72, 128–133, 217–222 and 245–249). All these regions contain insertions. Only the region of residues 69–72 is located in the vicinity of the active site. In the thermophilic enzyme the region of residues 141–146 is the only one with higher flexibility and it also contains an insertion. In addition, there was a difference in the RMSF profile of residues 315–327 in Xyl_P (corresponding to residues 311–329 in Xyl_T).

Essential dynamics revealed similar modes of motion in both studied xylanases despite a relatively low homology. Movements along the first eigenvector (Fig. 4) were characterized by opening of the active site groove. In the psychrophilic enzyme (Xyl_P) large movements of loops of residues 66–72 and 375–379 were also associated with the first eigenvector. The loop of residues 69–72 was observed as being more flexible from RMSF profiles and contains an insertion in Xyl_P. These loops cover the active site groove. Movements of other loops covering the active site (residues 267–274 and 335–339 of Xyl_P) are associated with the first eigenvector. The second eigenvector corresponds to a twisting of the whole $(\alpha/\alpha)_6$ barrel. Movements associated with both eigenvectors are enhanced in the structure of the psychrophilic enzyme.

Overall flexibilities

Overall flexibilities were calculated as averaged RMSF for separated 50 ps windows as well as over a whole

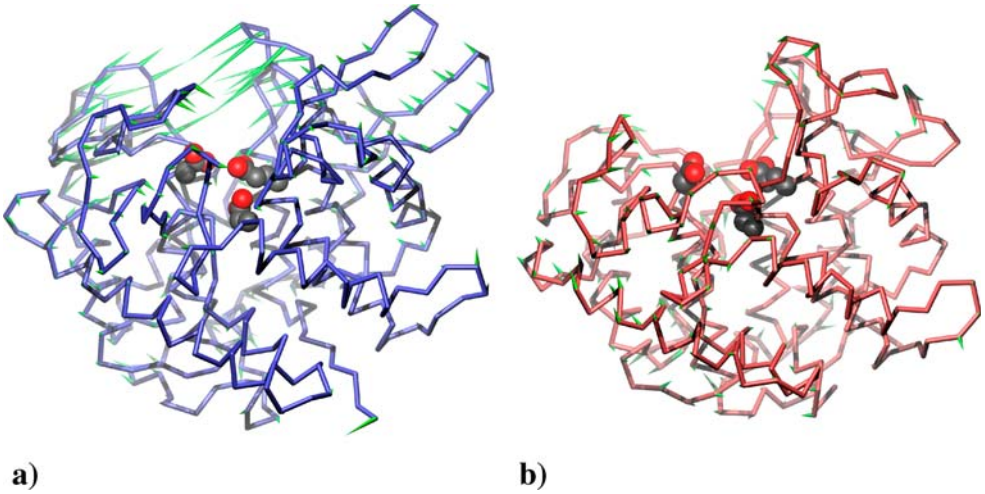

Fig. 4 Collective motions associated with the first eigenvector in structures of xylanases. Time averaged C^{α} traces are illustrated. (**a**) the cold-active enzyme in blue. (**b**) the thermophilic enzyme in red. Side chains of active site residues are shown as spheres. Collective motions associated with the first eigenvector are showed as green cones. These cones represent a product of the first eigenvector and the first eigenvalue (multiplied by a factor of two to make the figure more illustrative). Note that opening/closing of the active site loop of the cold-active enzyme is enhanced

production trajectory. The advantage of the former analysis is the fact that confidence intervals can be calculated. The disadvantage is that movements in time-scales longer than ~50 ps are not addressed. The results are illustrated in Fig. 2f. Average RMSF values calculated in 50 ps windows were in the range 0.05–0.07 nm. Except for α-amylases, the flexibility of the cold-active enzyme of a pair was higher than that of its meso- or thermophilic counterpart. However, differences between flexibilities fell within the 95% confidence interval. The higher flexibility of the mesophilic α-amylase could be explained by the presence of flexible insertions in the structure of the porcine enzyme (Amy_M). The same trend (higher flexibilities of cold-active enzymes except for α-amylase) was present and even enhanced in RMSF profiles calculated for whole production trajectories.

Correlation between flexibilities of corresponding residues

Calculation of overall averaged RMSF values does not necessarily indicate a structural role for individual amino acid residues. Hence a protein with large loop regions is interpreted as being more flexible although this flexibility is likely to play a small role in catalysis and stability. Therefore, the relationship between the flexibility of cold-active and meso- or thermophilic enzymes was examined using a structure-structure alignment generated by the CE method [39]. Each residue was represented as a point in an x-y plot, where the value on x-axis was the flexibility of a C^{α} atom in the cold-active enzyme and the value on y-axis was the flexibility of an equivalent C^{α} atom in the meso- or thermophilic enzyme. Residues in insertions were omitted. Regression coefficients were calculated by fitting x-y plots using the relationship:

$$RMSF_{meso/thermophile} = A \cdot RMSF_{psychrophile}$$

Therefore a regression coefficient lower than one indicates a higher flexibility of the cold-active enzyme. Regression coefficients A were calculated for RMSF values obtained in 50 ps windows, as well as for whole production trajectories. An example of this plot is shown in Fig. 5a (and as supplementary material for the other enzyme pairs). The calculated regression coefficients are illustrated in Fig. 5b. All regression coefficients were lower than one, demonstrating that all cold-active enzymes were more flexible (for flexibility defined by regression coefficients calculated on non-loop regions) than their meso- or thermophilic counterparts. Regression coefficients were generally smaller if calculated for whole production trajectories, so the higher flexibility of cold-active enzymes is related to motions in rather longer time-scales. The fact that the regression coefficient of α-amylase is lower than one, but, at the same time, the flexibility calculated as averaged RMSF is higher for the mesophilic enzyme, could be explained by the presence of flexible insertions in the mesophilic α-amylase. Note that all insertions were omitted in the regression analysis.

Flexibility as a function of temperature

Molecular dynamics was simulated for six temperatures between 280 and 330 K for both xylanases. Despite the fact that the experimental melting temperature of the cold-active xylanase Xyl_P is 322 K [1] (i.e. within the range of temperatures used in simulations), the enzyme cannot undergo a significant temperature unfolding within the relatively short time-scale of the simulation. Durations of these simulations were 1 400 ps (1 200 ps of production phase). Overall flexibilities, calculated as average RMSF, are illustrated in Fig. 6 for 50 ps windows (Fig. 6a) as well as for full production trajectories (Fig. 6b). Flexibilities increased with temperature as expected. Flexibility of the cold-active xylanase (Xyl_P) was always higher than that of thermophilic xylanase (Xyl_T) at any given temperature.

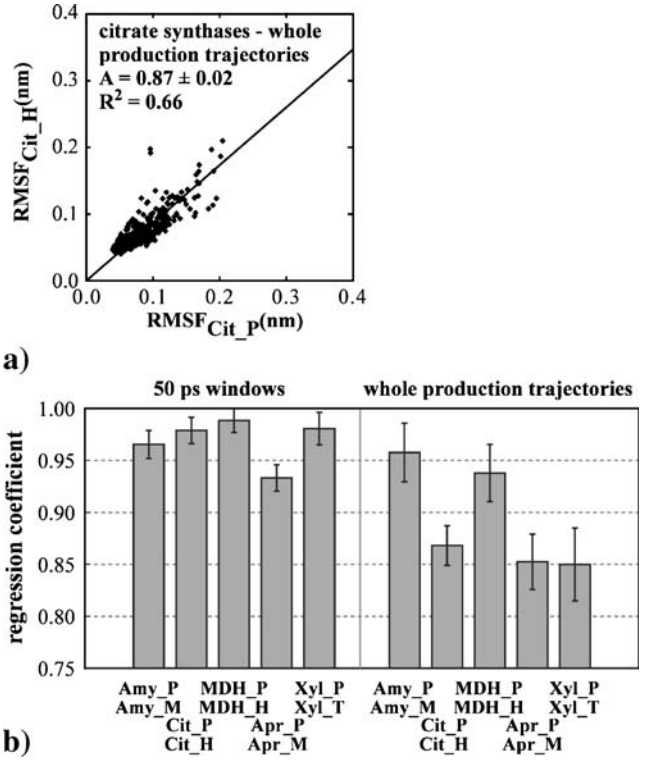

Fig. 5 Correlations of flexibilities of corresponding residues. (**a**) an example of correlation between flexibility of corresponding residues in the cold-active citrate synthase and the hyperthermophilic citrate synthase. (**b**) RMSF values calculated either in 50 ps windows or for whole production trajectories were compared for corresponding residues in the two enzymes. A value of regression coefficient lower than one indicates that flexibility of the cold-active enzyme is higher

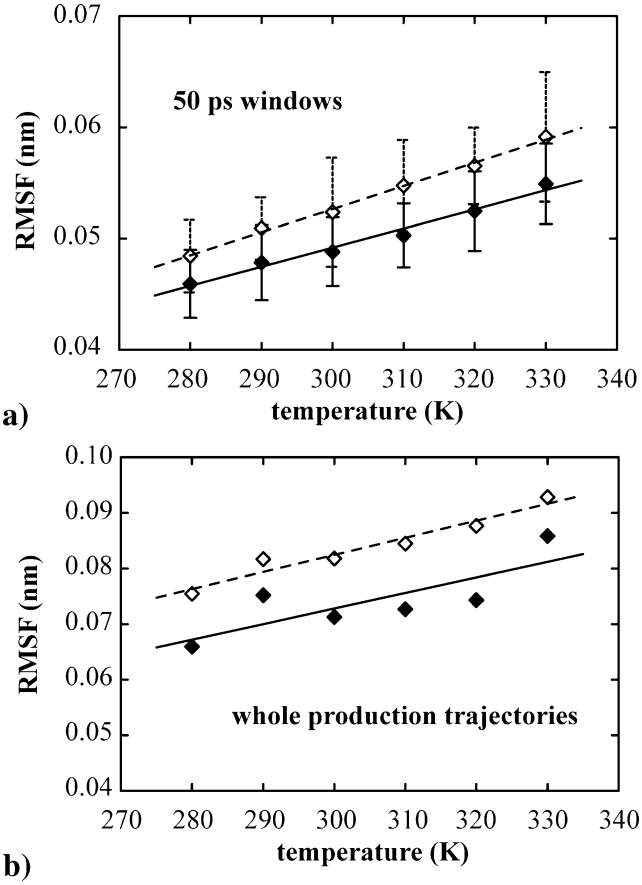

Fig. 6 Flexibility of the cold-active xylanase (*Pseudoalteromonas haloplanktis*, open squares and dashed lines) and thermophilic (*Clostridium thermocellum*, filled squares, solid lines) as a function of temperature. Flexibility was calculated either in 50 ps windows (**a**) or for whole production trajectories (**b**). The slope of flexibility as a function of temperature was higher for cold-active xylanase ($(21\pm2)\cdot10^{-5}$ nm/K) than for thermophilic xylanase ($(17\pm2)\cdot10^{-5}$ nm/K) for flexibility calculated in 50 ps windows. Confidence intervals are indicated by error bars for flexibilities calculated in 50 ps windows

There was a strong linear correlation between flexibility and temperature for both enzymes, especially for flexibility calculated in 50 ps windows. Interestingly, flexibilities are approximately the same at the apparent optimal temperatures of both enzymes. The slope of flexibility as a function of temperature was higher for cold-active xylanase ($(21\pm2)\cdot10^{-5}$ nm/K) than for thermophilic xylanase ($(17\pm2)\cdot10^{-5}$ nm/K) for flexibility calculated in 50 ps windows. The higher value of the slope for the cold-active enzyme is in agreement with trends observed by in vivo neutron scattering studies on whole cell samples of organisms adapted to different temperatures [55].

Essential dynamics data was also analysed for trajectories of xylanases calculated for different temperatures. This analysis showed that plots illustrating projection of a trajectory on the second versus projection on the first eigenvector as well as projection on the third versus projection on the first eigenvector calculated for simulations at different temperatures were similar for all temperatures and both enzymes (see supplementary material). In agreement with study of Lazaridis [36], we observed that modes of motions of a protein are analogous at different temperatures. On the other hand, contrary to the study of Lazaridis, we observed that essential motions are also analogous for homologous proteins.

Discussion

Overall, the results indicate that elevated conformational flexibility is a common trend in cold-active enzymes. Moreover, this elevated flexibility occurs over time-scales that can be achieved by molecular dynamics simulation. On the other hand, this enhanced flexibility is not so prominent as often supposed, at least in achieved time-scales. Flexibility profiles show that a difference between flexibilities of two enzymes depends strongly on a level of sequence identity. Amino acid residues belonging to insertions between compared proteins are generally very flexible in both cold-active enzymes as well as in enzymes from meso-

or thermophilic sources. However, residues within the protein core generally show higher flexibility in cold-active enzymes if compared with core residues of meso- or thermophilic enzymes. The idea of elevated overall flexibility in cold-active enzymes was supported by a common trend in correlation of flexibilities. Tehei and coworkers compared the flexibility of whole-cell samples of psychrophilic, mesophilic and thermophilic organisms using neutron scattering experiments [55]. They observed that the slope of global mean square atomic displacement ($<u^2>$) as a function of temperature is highest for the psychrophile, reduced for the mesophile and even lower for the thermophile. In our study the profile of overall flexibility of xylanases as a function of temperature showed that flexibilities are approximately the same at the apparent optimal temperature of each enzyme. The slope of flexibility as a function of temperature is also higher for the cold-active enzyme, which agrees with the results of Tehei [55].

It is possible to trace differences in flexibilities of certain regions between two homologous enzymes. However, evidence supporting the idea that elevated flexibility of cold-active enzymes is localized to the active site would require longer trajectories to provide a statistical insight. Essential dynamics analysis detected several collective motions to be enhanced in cold-active enzymes. A spatial character of these motions indicates that they might play an important role in catalysis. This is particularly the case for xylanases (Fig. 4), where opening and closing of the active site groove is enhanced in the cold-active enzyme. On this basis, we anticipate that amplitudes and/or rates of these motions play an important role in adaptation of enzymes to function at low temperature. This role seems to be more important than a simple flexibility defined as RMSF. Tracing these motions and performing a mutagenesis of residues that control these motions (e.g. "hinge" regions) seems to be a viable strategy in enzyme engineering. Nevertheless, flexibility-activity and flexibility-stability relationships remain an issue.

One possible explanation is that flexibility plays an important role in enzymatic reactions where the flexibility-related step (e.g. opening/closing of the active site) is the rate-limiting step of an enzymatic reaction. If the rate-limiting step is substrate turnover, then flexibility of the protein seems to be less important. Some insight is provided by studies where a protein is cooled below its transition temperature and all anharmonic motions are ceased [56–59]. Provided that protein dynamics plays an important role in enzyme catalysis, a certain jump transition of activity as a function of temperature is expected when an enzyme is cooled bellow its transition temperature because anharmonic motions in the protein structure are ceased. There are examples of proteins for which such transitions in a function were observed; for example the photocycle of bacteriorhodopsin [56] and in the interaction of ribonuclease A with ligand [57]. On the other hand, enzymatic activity of glutamate dehydrogenase [58] and xylanase [59] (both from thermophilic species) did not show any transition in activity and followed an Arrhenius equation. Therefore, flexibility could be critically involved only in certain types of reactions.

Adenylate kinase is an example of an enzyme for which the rate-limiting step was proved to be related to flexibility [60]. Wolf-Watz and co-workers showed that opening and closing of active-site lids is the rate-limiting step of the reaction in a mesophilic as well as a thermophilic adenylate kinase [60]. Using NMR relaxation they showed that reduced activity of the thermophilic enzyme is caused by a slower rate of opening and closing of the active site [60]. Our results also indicate that conformational motions involved in active-site opening and closing differ between enzymes adapted to different temperatures. On the other hand, Wolf-Watz proved that opening and closing of the active site of the enzyme is the rate-limiting step. Detailed kinetic measurements are necessary to test this concept for enzymes involved in this study. The role of flexibility has to be carefully evaluated also in enzymes where the rate-limiting step is a substrate turnover step, rather than a step directly related to flexibility. Adaptation of enzymes to high or low temperatures are comprised of complex changes in enzyme dynamics and these changes have to be characterized by biophysical methods, kinetic measurements, mutagenesis and other techniques. Comparative molecular dynamics simulation provides a tool to select certain modes of motion or regions as candidates for rationalizing structure-activity and structure-stability relationships.

Acknowledgment This work was supported by the Academy of Sciences of the Czech Republic (GAAV KJB 500500512) and the Ministry of Education, Youth and Sports (MSM 6046137305). The authors would like to acknowledge colleagues from the Department of Biochemistry and Microbiology, Institute of Chemical Technology Prague who have lent their personal computers during holiday periods for performing some of the computations presented herein. They are listed on the following web site: biomikro.vscht.cz/groups/lab211/holiday.

References

1. Collins T, Meuwis MA, Gerday C, Feller G (2003) J Mol Biol 328:419–428 DOI 10.1016/S0022-2836(03)00287-0
2. Russell NJ (1997) Comp Biochem Physiol A Physiol 118:489–493
3. Aghajari N, Feller G, Gerday C, Haser R (1998) Structure 6:1503–1516 DOI 10.1016/S0969-2126(98)00149-X
4. Russell RJ, Gerike U, Danson MJ, Hough DW, Taylor GL (1998) Structure 6:351–361 DOI 10.1016/S0969-2126(98)00037-9
5. Kim SY, Hwang KY, Kim SH, Sung HC, Han YS, Cho Y (1999) J Biol Chem 274:11761–11767

6. Aghajari N, van Petegem F, Villeret V, Chessa JP, Gerday C, Haser R, van Beeumen J (2003) Proteins 50:636–647 DOI 10.1002/prot.10264
7. van Petegem F, Collins T, Meuwis MA, Gerday C, Feller G, van Beeumen J (2003) J Biol Chem 278:7531–7539 DOI 10.1074/jbc.M206862200
8. Arnorsdottir J, Kristjansson MM, Ficner R (2005) FEBS J 272:832–845 DOI 10.1111/j.1742-4658.2005.04523.x
9. Alvarez M, Zeelen JP, Mainfroid V, Rentier-Delrue F, Martial JA, Wyns L, Wierenga RK, Maes D (1998) J Biol Chem 273:2199–2206
10. Bae E, Phillips GN Jr (2004) J Biol Chem 279:28202–28208 DOI 10.1074/jbc.M401865200
11. Gianese G, Bossa F, Pascarella S (2002) Proteins 47:236–249 DOI 10.1002/prot.10084
12. Gianese G, Argos P, Pascarella S (2001) Protein Eng 14:141–148
13. Saunders NF, Thomas T, Curmi PM, Mattick JS, Kuczek E, Slade R, Davis J, Franzmann PD, Boone D, Rusterholtz K, Feldman R, Gates C, Bench S, Sowers K, Kadner K, Aerts A, Dehal P, Detter C, Glavina T, Lucas S, Richardson P, Larimer F, Hauser L, Land M, Cavicchioli R (2003) Genome Res 13:1580–1588 DOI 10.1101/gr.1180903
14. Zavodszky P, Kardos J, Svingor, Petsko GA (1998) Proc Natl Acad Sci USA 95:7406–7411
15. Shoichet BK, Baase WA, Kuroki R, Matthews BW (1995) Proc Natl Acad Sci USA 92:452–456
16. Beadle BM, Shoichet BK (2002) J Mol Biol 321:285–296 DOI 10.1016/S0022-2836(02)00599-5
17. Olufsen M, Smalas AO, Moe E, Brandsdal BO (2005) J Biol Chem 280:18042–18048 DOI 10.1074/jbc.M500948200
18. Taverna DM, Goldstein RA (2002) Proteins 46:105–109 DOI 10.1002/prot.10016
19. Heimstad ES, Hansen LK, Smalas AO (1995) Protein Eng 8:379–399
20. Brandsdal BO, Heimstad ES, Sylte I, Smalas AO (1999) J Biomol Struct Dyn 17:493–506
21. Brandsdal BO, Aqvist J, Smalas AO (2001) Protein Sci 10:1584–1595
22. Gorfe AA, Brandsdal BO, Leiros HK, Helland R, Smalas AO (2000) Proteins 40:207–217 DOI 10.1002/(SICI)1097-0134(20000801)40:2<207::AID-PROT40>3.0.CO;2-U
23. Brandsdal BO, Smalas AO, Aqvist J (2001) FEBS Lett 499:171–175 DOI 10.1016/S0014-5793(01)02552-2
24. Moe E, Leiros I, Riise EK, Olufsen M, Lanes O, Smalas A, Willassen NP (2004) J Mol Biol 343:1221–1230 DOI 10.1016/j.jmb.2004.09.004
25. D'Amico S, Gerday C, Feller G (2002) J Biol Chem 277:46110–46115 DOI 10.1074/jbc.M207253200
26. Mavromatis K, Feller G, Kokkinidis M, Bouriotis V (2003) Protein Eng 16:497–503
27. Mavromatis K, Tsigos I, Tzanodaskalaki M, Kokkinidis M, Bouriotis V (2002) Eur J Biochem 269:2330–2335
28. Narinx E, Baise E, Gerday C (1997) Protein Eng 10:1271–1279
29. Ohtani N, Haruki M, Morikawa M, Kanaya S (2001) Protein Eng 14:975–982
30. Agarwal PK (2006) Microb Cell Fact 5 DOI 10.1186/1475-2859-5-2
31. McCammon JA, Gelin BR, Karplus M (1977) Nature 276:585–590 DOI 10.1038/267585a0
32. Hayward JA, Finney JL, Daniel RM, Smith JC (2003) Biophys J 85:679–685
33. Stocker U, Spiegel K, van Gunsteren WF (2000) J Biomol NMR 18:1–12 DOI 10.1023/A:1008379605403
34. Wintrode PL, Zhang D, Vaidehi N, Arnold FH, Goddard WA III (2003) J Mol Biol 327:745–757 DOI 10.1016/S0022-2836(03)00147-5
35. Grottesi A, Ceruso MA, Colosimo A, Di Nola A (2002) Proteins 46:287–294 DOI 10.1002/prot.10045
36. Lazaridis T, Lee I, Karplus M (1997) Protein Sci 6:2589–2605
37. Amadei A, Linssen AB, Berendsen HJ (1993) Proteins 17:412–425 DOI 10.1002/prot.340170408
38. Berman HM, Battistuz T, Bhat TN, Bluhm WF, Bourne PE, Burkhardt K, Feng Z, Gilliland GL, Iype L, Jain S, Fagan P, Marvin J, Padilla D, Ravichandran V, Schneider B, Thanki N, Weissig H, Westbrook JD, Zardecki C (2002) Acta Cryst D58:899–907 DOI 10.1107/S0907444902003451
39. Guda C, Lu S, Scheeff ED, Bourne PE, Shindyalov IN (2004) Nucleic Acids Res 32:W100–W103 DOI 10.1093/nar/gkh464
40. Sali A, Blundell TL (1993) J Mol Biol 234:779–815 DOI 10.1006/jmbi.1993.1626
41. Canutescu AA, Shelenkov AA, Dunbrack RL Jr (2003) Protein Sci 12:2001–2014
42. Feller G, Bussy O, Houssier C, Gerday C (1996) J Biol Chem 271:23836–23841
43. Ravaud S, Gouet P, Haser R, Aghajari N (2003) J Bacteriol 185:4195–4203 DOI 10.1128/JB.185.14.4195-4203
44. Berendsen HJC, Postma JPM, van Gunsteren WF, Hermans J (1981) Interaction models for water in relation to protein hydration. In: Pullman B (ed) Intermolecular forces
45. Berendsen HJC, van der Spoel D, van Drunen R (1995) Comp Phys Comm 91:43–56 DOI 10.1016/0010-4655(95)00042-E
46. Lindahl E, Hess B, van der Spoel D (2001) J Mol Mod 7:306–317 DOI 10.1007/s008940100045
47. Berendsen HJC, Postma JPM, DiNola A, Haak JR (1984) J Chem Phys 81:3684–3690 DOI 10.1063/1.448118
48. Parrinello M, Rahman A (1981) J Appl Phys 52:7182–7190 DOI 10.1063/1.328693
49. Hess B, Bekker H, Berendsen HJC, Fraaije JGEM (1997) J Comp Chem 18:1463–1472 DOI 10.1002/(SICI)1096-987X(199709)18:12<1463::AID-JCC4>3.0.CO;2-H
50. Fan H, Mark AE (2003) Proteins 53:111–120 DOI 10.1002/prot.10496
51. Rost B (2002) Curr Opin Struct Biol 12:409–416 DOI 10.1016/S0959-440X(02)00337-8
52. Fitter J, Heberle J (2000) Biophys J 79:1629–1637
53. Roccatano D, Mark AE, Hayward S (2001) J Mol Biol 310:1039–1054 DOI 10.1006/jmbi.2001.4808
54. Kurz LC, Drysdale G, Riley M, Tomar MA, Chen J, Russell RJ, Danson MJ (2000) Biochemistry 39:2283–2297 DOI 10.1021/bi991982r
55. Tehei M, Franzetti B, Madern D, Ginzburg M, Ginzburg BZ, Giudici-Orticoni MT, Bruschi M, Zaccai G (2004) EMBO Rep 5:66–77 DOI 10.1038/sj.embor.7400049
56. Ferrand M, Dianoux AJ, Petry W, Zaccai G (1993) Proc Natl Acad Sci USA 90:9668–9672
57. Rasmussen BF, Stock AM, Ringe D, Petsko GA (1992) Nature 357:423–424 DOI 10.1038/357423a0
58. Daniel RM, Smith JC, Ferrand M, Hery S, Dunn R, Finney JL (1998) Biophys J 75:2504–2507
59. Dunn RV, Reat V, Finney J, Ferrand M, Smith JC, Daniel RM (2000) Biochem J 346:355–358
60. Wolf-Watz M, Thai V, Henzler-Wildman K, Hadjipavlou G, Eisenmesser EZ, Kern D (2004) Nat Struct Mol Biol 11:945–949 DOI 10.1038/nsmb821
61. Qian M, Nahoum V, Bonicel J, Bischoff H, Henrissat B, Payan F (2001) Biochemistry 40:7700–7709 DOI 10.1021/bi0102050
62. Russell RJ, Ferguson JM, Hough DW, Danson MJ, Taylor GL (1997) Biochemistry 36:9983–9994 DOI 10.1021/bi9705321
63. to be published
64. Baumann U, Wu S, Flaherty KM, McKay DB (1993) EMBO J 12:3357–3364
65. Alzari PM, Souchon H, Dominguez R (1996) Structure 4:265–275 DOI 10.1016/S0969-2126(96)00031-7